NJC

PAPER

View Article Online
View Journal | View Issue

Open Access Article. Published on 05 January 2017. Downloaded on 8/1/2025 11:28:32 AM.
This article is licensed under a Creative Commons Attribution-NonCommercial 3.0 Unported Licence.

Cite this: *New J. Chem.*, 2017, **41**, 1670

Water-soluble hybrid materials based on $\{Mo_6X_8\}^{4+}$ (X = Cl, Br, I) cluster complexes and sodium polystyrene sulfonate†

Ekaterina V. Svezhentseva,[ab] Anastasiya O. Solovieva,[c] Yuri A. Vorotnikov,[a] Olga G. Kurskaya,[d] Konstantin A. Brylev,[ab] Alphiya R. Tsygankova,[ab] Mariya V. Edeleva,[e] Svetlana N. Gyrylova,[d] Noboru Kitamura,[f] Olga A. Efremova,*[g] Michael A. Shestopalov,*[abcd] Yuri V. Mironov[ab] and Alexander M. Shestopalov[d]

Received 4th November 2016,
Accepted 4th January 2017

DOI: 10.1039/c6nj03469a

rsc.li/njc

The development of water-soluble forms of octahedral molybdenum clusters $\{Mo_6X_8\}^{4+}$ (X = Cl, Br, I) is strongly motivated by the tremendous potential that these complexes have for biological applications, namely as agents for bioimaging and photodynamic therapy. In this work, we report the first water-soluble hybrid materials, which represent sodium polystyrene sulfonate doped by molybdenum clusters, and the evaluation of their photophysical and biological properties (dark and photoinduced cytotoxicity and cellular uptake) with the use of cervical cancer (HeLa) and human epidermoid larynx carcinoma (Hep-2) cell-lines as models.

Introduction

Octahedral molybdenum cluster complexes having a $\{Mo_6X_8\}^{4+}$ core, where X is a halogen atom (Cl, Br or I) (Fig. 1), have recently attracted a lot of attention from materials scientists due to their outstanding photophysical properties. Particularly, such cluster complexes demonstrate emission within the biological tissue window (550–900 nm) and high (up to ~0.7) photoluminescence quantum yields.[1–4] Moreover, the hexamolybdenum clusters are also efficient singlet oxygen generators.[5–8] Therefore, $\{Mo_6X_8\}^{4+}$-based complexes are potentially outstanding luminophores and photosynthesisers for biological applications such as bioimaging and photodynamic therapy, respectively. Unfortunately, apart from several exceptions, the majority of known hexamolybdenum cluster complexes are poorly soluble in water, while few known examples of water-soluble Mo_6 cluster complexes tend to hydrolyse easily in the presence of water.[5,9,10] Poor solubility and stability of the complexes in water hinder the studies on their biological activity and consequently any biomedical applications.

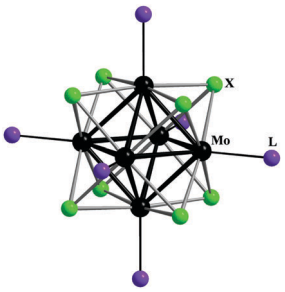

Fig. 1 The general structure of octahedral cluster complexes $[\{Mo_6X_8\}L_6]^n$, where X is either Cl, Br or I and L is either an organic or inorganic terminal ligand.

In order to tackle this obstacle we recently developed an approach, in which hexamolybdenum cluster complexes were supported by inert matrices, such as SiO_2 nanoparticles,[11–14] polystyrene microparticles[7,15–17] and metal–organic frameworks,[9,18,19] which are known to build stable suspensions in water.

Such an approach allowed us to study some biological properties (*e.g.* dark cytotoxicity and photoinduced cytotoxicity) of Mo_6 cluster containing polymer materials. It is obvious though that the above approach does not produce materials,

[a] *Nikolaev Institute of Inorganic Chemistry SB RAS, 3 Acad. Lavrentiev Ave., 630090 Novosibirsk, Russian Federation. E-mail: shtopy@niic.nsc.ru; Fax: +7 383 330 94 89; Tel: +7 383 330 92 53*
[b] *Novosibirsk State University, 2 Pirogova Str., 630090 Novosibirsk, Russian Federation*
[c] *Scientific Institute of Clinical and Experimental Lymphology, 2 Timakova Str., 630060 Novosibirsk, Russian Federation*
[d] *Research Institute of Experimental and Clinical Medicine, 2 Timakova Str., 630060 Novosibirsk, Russian Federation*
[e] *Vorozhtsov Novosibirsk Institute of Organic Chemistry SB RAS, 9 Acad. Lavrentiev Ave, 630090 Novosibirsk, Russian Federation*
[f] *Department of Chemistry, Faculty of Science, Hokkaido University, 060-0810 Sapporo, Japan*
[g] *Department of Chemistry, University of Hull, Cottingham Road, Hull, HU6 7RX, UK. E-mail: o.efremova@hull.ac.uk; Tel: +44 (0)1482 465417*

† Electronic supplementary information (ESI) available: FTIR spectra, UV-Vis spectra, ICP data, emission spectra and FACS data. See DOI: 10.1039/c6nj03469a

 This journal is © The Royal Society of Chemistry and the Centre National de la Recherche Scientifique 2017

Open Access Article. Published on 05 January 2017. Downloaded on 8/1/2025 11:28:32 AM.
This article is licensed under a Creative Commons Attribution-NonCommercial 3.0 Unported Licence.

where hexamolybdenum cluster anions would be dissolved in water, which could be valuable in the context of increasing singlet oxygen generation efficiency and corresponding photo-induced toxicity. Indeed, in our previous work we showed that the efficiency of singlet oxygen generation was strongly dependent on the size of the particles: the higher specific surface area, the more efficient the singlet oxygen generation.[11]

In this work, we demonstrate a new approach to deliver hexamolybdenum cluster complexes in an aqueous phase. In this method, highly water-soluble anionic polymer sodium polystyrene sulfonate (PSS) was used to bind the $\{Mo_6X_8\}^{4+}$ (X = Cl, Br or I) cluster complexes in order to dissolve them in aqueous media. The cytotoxicity of the obtained hybrid materials $\{Mo_6X_8\}$@PSS was studied by MTT assay in cervical cancer (HeLa) and human epidermoid larynx carcinoma (Hep-2) cells, while the internalisation of the cluster complexes from the solutions into HeLa cells was traced by flow cytometry.

Results and discussion

Preparation and characterisation of PSS and $\{Mo_6X_8\}^n$@PSS

To develop water-soluble material containing $\{Mo_6X_8\}^{4+}$, we have chosen a strategy, in which metal clusters are bonded to a highly water-soluble polymer matrix that has a high molecular weight, so that the binding of the cluster complex to the polymer would not affect significantly the solubility of the final hybrid material. Sodium polystyrene sulfonate (PSS) is a cheap, easy to prepare and highly soluble polymer matrix. It is also well-known for its ability to bind efficiently metal cations and cationic complexes due to the plethora of sulfonate groups,[20] which led to PSS being approved for medical treatment of hyperkalemia in some countries.[21]

Cluster complexes of composition $[\{Mo_6X_8\}(NO_3)_6]^{2-}$ (X = Cl, Br or I) were selected as convenient sources of $\{Mo_6X_8\}^{4+}$ due to their well-recognised lability associated with easy substitution of apical NO_3^- ligands by other groups. Indeed, this ability of the nitrato cluster complexes was earlier exploited to develop new complexes[17] as well as hybrid materials with thiol-functionalised polystyrene[15,17] and silica particles.[11,12]

The PSS polymer of high molecular weight was obtained according to a standard free radical polymerisation reaction of 4-styrenesulfonic acid sodium salt in an aqueous solution initiated by sodium peroxodisulfate. According to elemental analysis the obtained polymer contained two water molecules per monomeric unit. The molecular mass (M_n) of PSS determined by size exclusion chromatography (SEC) was found to be 2.2 MDa.

Water-soluble molybdenum cluster doped materials $\{Mo_6X_8\}^n$@PSS (where n = 1, 5, 10 and 100 refers to the loading of cluster complexes $(Bu_4N)_2[\{Mo_6X_8\}(NO_3)_6]$ (X = Cl, Br or I) in milligrams per 100 mg of initial PSS) were obtained by impregnation of solid PSS with acetone solutions of $(Bu_4N)_2[\{Mo_6X_8\}(NO_3)_6]$ at concentrations of 0.2, 1, 2 or 20 mg mL^{-1}. After the reactions, the yellow-coloured solids (namely light yellow, yellow and dark yellow for X = Cl, Br and I, respectively) were separated by centrifugation, washed with an excess of acetone to remove any unbounded metal cluster complex and dried in air. A UV-vis study of $\{Mo_6X_8\}^n$@PSS aqueous solutions has indeed shown enhanced absorbance in the wavelength region 270–450 nm (Fig. S1–S3, ESI†) due to the presence of the yellow metal cluster complexes.

The data of the FTIR and elemental (CHNS) analyses of $\{Mo_6X_8\}^n$@PSS hybrids showed that all NO_3^- ligands and tetra-*n*-butyl ammonium cations were removed upon the reactions of $(Bu_4N)_2[\{Mo_6X_8\}(NO_3)_6]$ with PSS (Fig. S4–S7, ESI†). This observation suggests that nitrato ligands were substituted by the sulfonate groups present in PSS and water molecules and removed as $NaNO_3$ and Bu_4NNO_3. Such substitution of nitrato ligands in the impregnation reaction of a polymer material with a solution of $(Bu_4N)_2[\{Mo_6X_8\}(NO_3)_6]$ was previously observed on thiol-functionalised polystyrene microspheres.[15,17]

To demonstrate the importance of the labile nitrato ligands in the reaction of PSS with hexamolybdenum cluster complexes, we also tested $(Bu_4N)_2[\{Mo_6I_8\}(OOCCH_3)_6]$ (obtained according to ref. 1) under the same conditions and even at increased temperature. Indeed, we observed that PSS did not acquire the yellow colour of the cluster complex at all (see Fig. S8, ESI†) as well as ICP data did not show any Mo in the sample.

According to the ICP data of $\{Mo_6X_8\}^n$@PSS, the content of molybdenum in the polymer increased, while the content of sodium decreased with the increase of the value n. Notably, the content of both elements was significantly lower than the theoretical content, especially for the samples $\{Mo_6X_8\}^{100}$@PSS, for which the content of the metals was almost the same as for $\{Mo_6X_8\}^{10}$@PSS (Fig. S9–S11, ESI†). The real loading of the cluster in the samples $\{Mo_6X_8\}^{100}$@PSS estimated from both ICP and elemental analyses was about one cluster unit per 150 ± 10 monomer units. All further characterisations were performed using the samples $\{Mo_6X_8\}^{100}$@PSS.

To evaluate the influence of the conjugation of the cluster complexes to PSS on hydrodynamic properties, we compared the SEC and viscometry data for an aqueous solution of neat PSS with those of $\{Mo_6I_8\}^{100}$@PSS. The molecular mass of the hybrid material $\{Mo_6I_8\}^{100}$@PSS as determined by SEC was 1.9 MDa, *i.e.* slightly lower than that determined for neat PSS. This decrease in molecular mass, although unexpected, is attributed to the use of poly(ethylene glycol) (PEO) standards, which can provide only relative values of M_n. Moreover, the M_n determined from SEC is largely dependent on the behaviour of the hybrid polymer in the eluent and therefore can deviate from the linear dependence. In particular, one can expect that the PSS polymer could form a more globular structure, when it is bonded to metal cluster complexes. Notably, the viscosity of both solutions was found to be the same (η_r = 3.7), which confirms the similarity of the molecular mass of the starting polymer and the derivative hybrid material.

Luminescence properties

Our earlier works demonstrate that the incorporation of molybdenum cluster complexes in polymer matrices can significantly affect the photophysical properties of the cluster unit, especially when the ligand environment of $\{Mo_6X_8\}^{4+}$ is changed.[15,17] Therefore, we recorded the emission spectra and determined the values

Open Access Article. Published on 05 January 2017. Downloaded on 8/1/2025 11:28:32 AM.
This article is licensed under a Creative Commons Attribution-NonCommercial 3.0 Unported Licence.

of photoluminescence quantum yield and lifetime for both aqueous solutions and solid samples of $\{Mo_6X_8\}^{100}$@PSS. The luminescence spectra are shown in Fig. 2 (powdered samples) and Fig. S11 and S12 (ESI†) (aerated and deaerated aqueous solutions), while the emission maximum wavelengths (λ_{em}), lifetimes (τ_{em}) and photoluminescence quantum yields (Φ_{em}) are summarised in Table 1.

There are two maxima in the emission spectra of $\{Mo_6X_8\}^{100}$@PSS: at ~420 and ~700 nm that correspond to the fluorescence of the PSS matrix and the phosphorescence of the cluster complex, respectively.

Similarly to the recently described materials $\{Mo_6X_8\}$@PS-SH (X = Cl, Br or I; PS-SH – thiol-modified polystyrene microbeads),[15] powdered samples of PSS doped by chloride and bromide clusters were characterised by noticeably lower values of τ_{em} and Φ_{em} than the one doped by $\{Mo_6I_8\}^{4+}$, while λ_{em} values gradually decreased in the order Cl > Br > I (Fig. 2 and Table 1).

We were unable to determine the photophysical characteristics of aqueous $\{Mo_6Cl_8\}^{100}$@PSS and $\{Mo_6Br_8\}^{100}$@PSS reliably, since both aerated and deaerated solutions of $\{Mo_6Cl_8\}^{100}$@PSS were not emissive at all, while the solutions of $\{Mo_6Br_8\}^{100}$@PSS showed only very poor luminescence (Fig. 2, 3 and Fig. S12, S13, ESI†). In contrast, an aqueous solution of $\{Mo_6I_8\}^{100}$@PSS showed appreciable red luminescence. As expected, the aerated aqueous of $\{Mo_6I_8\}^{100}$@PSS exhibited relatively weak emission, while in the argon-saturated solution the emission peak of the cluster complexes was noticeably higher (Fig. 2 and Fig. S12, S13, ESI†). Indeed, the observed luminescence quenching in an aerated solution can be explained by the interaction of molecular oxygen with the triplet excited state of the cluster unit.[2–4,17,22,23]

In comparison with the initial cluster complexes $(Bu_4N)_2[\{Mo_6X_8\}(NO_3)_6]$ in the solid state, the positions of the emission maxima of solid $\{Mo_6X_8\}^{100}$@PSS are 12 nm and 60 nm blue shifted for X = Cl and Br, respectively, while for X = I the shift is only 5 nm to the red region. Notably, in work[15] a similar trend of the emission maxima positions of materials $\{Mo_6Cl_8\}$@PS-SH was noticed (Table 1). This behaviour could be explained by the change in the apical ligand environment of the cluster, *i.e.* by

Table 1 Spectroscopic and photophysical data of initial clusters and $\{Mo_6X_8\}^{4+}$-based hybrid materials

Sample	λ_{em}, nm	τ_{em}, μs (A)	Φ_{em}
In solid state			
$(Bu_4N)_2[\{Mo_6Cl_8\}(NO_3)_6]$[15]	765	τ_1 = 17 (0.14) τ_2 = 9.3 (0.02) τ_3 = 1.9 (0.84)	<0.005
$(Bu_4N)_2[\{Mo_6Br_8\}(NO_3)_6]$[15]	785	τ_1 = 19 (0.25) τ_2 = 11 (0.20) τ_3 = 0.9 (0.55)	<0.01
$(Bu_4N)_2[\{Mo_6I_8\}(NO_3)_6]$[17]	666	τ_1 = 96 (0.71) τ_2 = 26 (0.29)	0.26
$(Bu_4N)_2[\{Mo_6Cl_8\}(OTs)_6]^2$	723	τ_1 = 228 (0.7) τ_2 = 174 (0.3)	0.34
$(Bu_4N)_2[\{Mo_6Br_8\}(OTs)_6]^2$	708	τ_1 = 185 (0.7) τ_2 = 86 (0.3)	0.29
$(Bu_4N)_2[\{Mo_6I_8\}(OTs)_6]^2$	662	τ_1 = 135 (0.6) τ_2 = 56 (0.4)	0.44
$\{Mo_6Cl_8\}$@PS-SH[15]	745	τ_1 = 34.4 (0.07) τ_2 = 7.7 (0.16) τ_3 = 0.68 (0.77)	<0.005
$\{Mo_6Br_8\}$@PS-SH[15]	730	τ_1 = 32.0 (0.14) τ_2 = 9.3 (0.32) τ_3 = 1.0 (0.54)	<0.005
$\{Mo_6I_8\}$@PS-SH[17]	677	τ_1 = 45 (0.15) τ_2 = 16 (0.40) τ_3 = 2.2 (0.45)	0.04
$\{Mo_6Cl_8\}^{100}$@PSS	753	τ_1 = 25 (0.08) τ_2 = 3.5 (0.31) τ_3 = 0.7 (0.61)	0.01
$\{Mo_6Br_8\}^{100}$@PSS	725	τ_1 = 10.6 (0.09) τ_2 = 1.3 (0.24) τ_3 = 0.2 (0.67)	0.01
$\{Mo_6I_8\}^{100}$@PSS	671	τ_1 = 74.8 (0.19) τ_2 = 30.8 (0.38) τ_3 = 3.5 (0.43)	0.03
In aqueous solution (deaerated)			
$\{Mo_6I_8\}^{100}$@PSS	718	τ_1 = 43.4 (0.83) τ_2 = 8.1 (0.17)	0.01

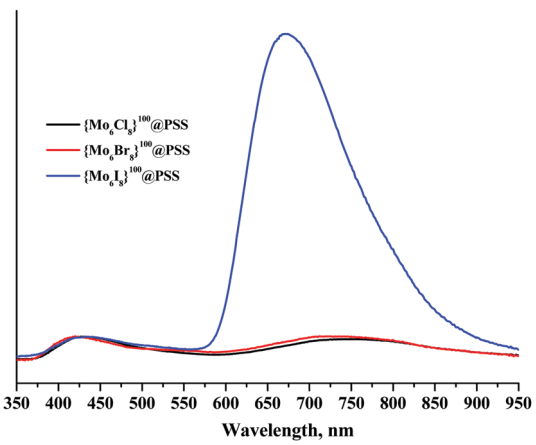

Fig. 2 Emission spectra of the powdered samples of $\{Mo_6X_8\}^{100}$@PSS normalised by the emission of PSS. The excitation wavelength was 355 nm.

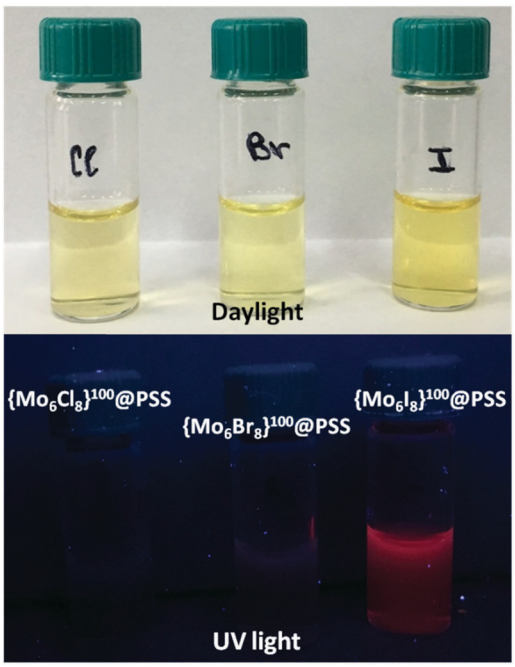

Fig. 3 Aqueous solutions of $\{Mo_6X_8\}^{100}$@PSS under daylight illumination (top) and UV-light (bottom) illumination.

 This journal is © The Royal Society of Chemistry and the Centre National de la Recherche Scientifique 2017

Open Access Article. Published on 05 January 2017. Downloaded on 8/1/2025 11:28:32 AM.
This article is licensed under a Creative Commons Attribution-NonCommercial 3.0 Unported Licence.

the substitution of nitrato ligands with sulfonate groups of the polymer matrix and water molecules. In contrast, in an earlier work, the emission profile of $[\{Mo_6I_8\}(OTs)_6]^{2-}$ (where OTs^- is *p*-toluene sulfonate) incorporated into the poly(methyl methacrylate) matrix did not significantly change from that of the starting cluster complex, since no substitution of the apical ligands took place in the latter case.[3] It should be also noted that the lifetimes and quantum yields of $\{Mo_6X_8\}^{100}$@PSS are significantly lower than those found for hexamolybdenum cluster complexes in a pure sulfonate ligand environment.[2,3] We believe that this is due to the presence of water molecules in the ligand environment of the cluster core in the $\{Mo_6X_8\}^{100}$@PSS materials. The quenching of photoluminescence by aqua-ligands *via* non-radiative relaxation associated with O–H vibrations is indeed well recognised in the literature.[5,24]

Cell viability, proliferation and cellular uptake of $\{Mo_6X_8\}^{100}$@PSS hybrids

The effect of PSS and $\{Mo_6X_8\}^{100}$@PSS hybrids on the viability of Hep-2 and HeLa cells was evaluated by MTT assay in the concentration range 3.2–3300 μg mL^{-1} (Fig. 4). The percentage of metabolically active cells was determined against the negative control. As expected, PSS demonstrated very low toxicity within the whole range of concentrations studied. Therefore, the half-maximum inhibitory concentrations (IC_{50}) of PSS for either cell line were not established. $\{Mo_6Cl_8\}^{100}$@PSS also showed relatively low toxicity – the IC_{50} value was not achieved within the studied concentration range in the case of both HeLa and Hep-2 cells. In contrast, materials doped by "heavier" cluster cores showed somewhat increased toxicity, but only for HeLa cells, with IC_{50} values equal to 1.3 ± 0.3 mg mL^{-1} (X = Br) and 0.37 ± 0.08 mg mL^{-1} (X = I).

The confocal microscopy imaging of both cell lines incubated with the solutions of $\{Mo_6X_8\}^{100}$@PSS (0.10 mg mL^{-1}) for 24 h has not registered any red emission of the cluster compounds within the cells.

Since the detection sensitivity of flow cytometry (FACS) is significantly higher than that of confocal microscopy,[25] we also analysed the cells by this technique. Indeed, FACS showed that the luminescence intensity of HeLa cells treated with $\{Mo_6Br_8\}^{4+}$ and $\{Mo_6I_8\}^{4+}$ doped materials increased, but only very slightly. However, in the case of Hep-2 cells the luminescence intensity of the cells treated with $\{Mo_6I_8\}^{100}$@PSS was significantly higher than that of the control cells (Fig. S14, ESI†).

Photoinduced cytotoxicity of $\{Mo_6X_8\}^{100}$@PSS hybrids

The singlet oxygen ($^1O_2$) generation ability of different photoluminescent octahedral metal cluster complexes and materials based on them was demonstrated in several studies.[5–7,11,24] We also recently demonstrated that cluster-doped silica nanoparticles showed photoinduced cytotoxicity associated with the generation of singlet oxygen.[12]

Since the FACS analysis demonstrated some uptake of the cluster-doped materials, we also evaluated the photoinduced cytotoxicity of $\{Mo_6X_8\}^{100}$@PSS hybrids in both cell cultures, HeLa and Hep-2, within the non-toxic concentration range 3.2–51.6 μg mL^{-1} (Fig. 5). According to our data, materials $\{Mo_6Br_8\}^{100}$@ PSS and $\{Mo_6I_8\}^{100}$@PSS demonstrated some photoinduced cytotoxicity towards HeLa cells: at the highest concentration, 51.6 μg mL^{-1}, the percentage of the living cells after photoirradiation for 30 min was ~70% for $\{Mo_6Br_8\}^{100}$@PSS and ~62% for $\{Mo_6I_8\}^{100}$@PSS. $\{Mo_6Cl_8\}^{100}$@PSS, however, did not show any appreciable phototoxicity, likely due to its poor photoluminescence properties.

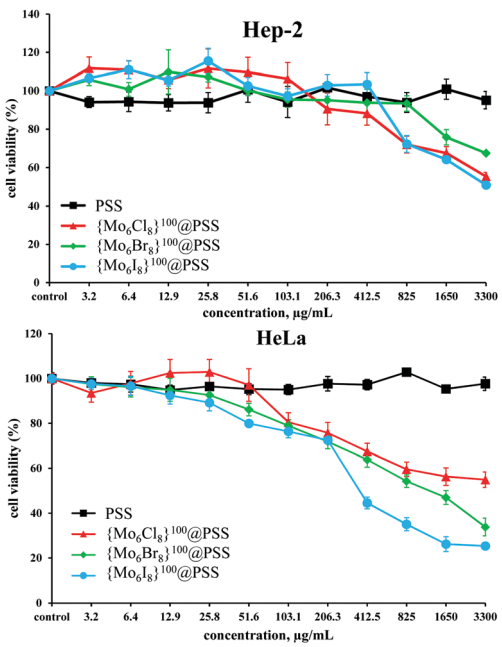

Fig. 4 Viability of Hep-2 (top) and HeLa (bottom) cells incubated with PSS and $\{Mo_6X_8\}^{100}$@PSS determined by MTT assay.

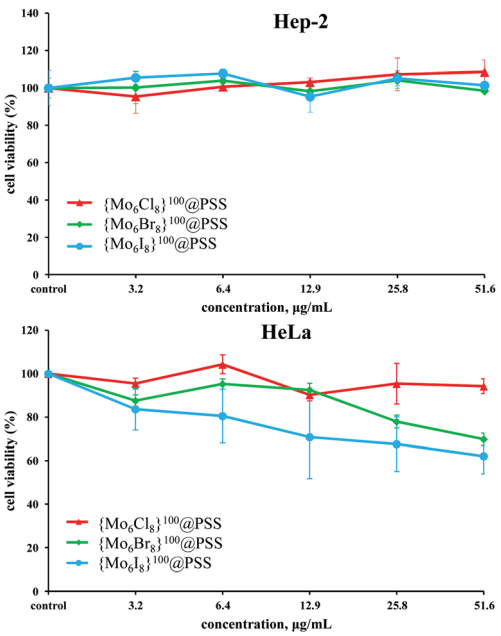

Fig. 5 Viability of Hep-2 (top) and HeLa (bottom) cells treated with $\{Mo_6X_8\}^{100}$@PSS after photoirradiation (λ = 400 nm, 30 min) determined by dual staining with Hoechst 33342/PI.

Open Access Article. Published on 05 January 2017. Downloaded on 8/1/2025 11:28:32 AM.
This article is licensed under a Creative Commons Attribution-NonCommercial 3.0 Unported Licence.

Surprisingly, in the case of Hep-2 cells even $\{Mo_6I_8\}^{100}$@PSS (one that was taken up well by the cells according to FACS) did not demonstrate any noticeable photoinduced cytotoxicity. This observation together with the noticeably higher IC_{50} values for the dark toxicity of $\{Mo_6X_8\}^{100}$@PSS clearly demonstrate higher resistance of Hep-2 cells to external influences in comparison with HeLa cells.

Experimental

Materials and methods

All reagents and solvents employed were commercially available and used as received without further purification. $(Bu_4N)_2[\{Mo_6X_8\}(NO_3)_6]$, where X = Cl, Br, I, were prepared according to the earlier described procedures.[17,26]

The CHNS elemental analyses were performed on a Euro-Vector EA3000 elemental analyser. The molybdenum content in all samples was determined on a high-resolution spectrometer iCAP-6500 (Thermo Scientific) with a cyclone-type spray chamber and "SeaSpray" nebulizer. The spectra were obtained by axial plasma viewing. Standard operating conditions of the ICP-AES system were as follows: power = 1150 W, injector inner diameter = 3 mm, carrier argon flow = 0.7 L min^{-1}, accessorial argon flow = 0.5 L min^{-1}, cooling argon flow = 12 L min^{-1}, number of parallel measurements = 3, and integration time = 5 s. Deionised water ($R \approx 18$ MΩ) was used to prepare sample solutions.

Preparation of sodium polystyrene sulfonate (PSS) by free radical polymerisation reaction

Sodium poly(4-styrenesulfonate) (PSS) was prepared in accordance with the literature procedure:[27,28] 10 g of 4-styrenesulfonic acid sodium salt hydrate and 10 mg of sodium persulfate were dissolved in 100 mL of water and purged with argon for 1 h. The reaction mixture was then sealed and kept for 24 h at 80 °C. The resultant viscous solution was slowly added to 1.5 L of ethanol under intense stirring. The obtained white fibrous PSS was separated from the mixture by decantation, washed with ethanol and dried at 70 °C. Yield: 9.1 g (91 wt%). Found: C 39.5, H 4.6, N 0.0, S 13.0. Calculated for $(CH_2CHC_6H_4SO_3Na{\cdot}2H_2O)_n$: C 39.7, H 4.6, N 0, S 13.2.

General procedure for immobilization of $(Bu_4N)_2[\{Mo_6X_8\}(NO_3)_6]$ (X = Cl, Br, I) into sodium polystyrene sulfonate – $\{Mo_6X_8\}^n$@PSS

All procedures were carried out at room temperature. Powdered $\{Mo_6X_8\}^n$@PSS (where n = 1, 5, 10 or 100 relates to the loading of cluster complexes $(Bu_4N)_2[\{Mo_6X_8\}(NO_3)_6]$ (X = Cl, Br or I) in milligrams per 100 mg of initial PSS) were obtained according to the following procedure: samples of solid PSS (100 mg) were stirred vigorously with 5 mL of acetone solutions containing $(Bu_4N)_2[\{Mo_6X_8\}(NO_3)_6]$ (1, 5, 10 or 100 mg). The reaction mixture was left overnight. The yellow coloured solid was then separated from the mother liquor by centrifugation (7700 rpm for 10 min), washed several times with acetone until the last washing solution remained colourless, once by ethanol and then dried at 70 °C.

For $\{Mo_6X_8\}^{100}$@PSS found: C 37.2, H 4.8, N 0, S 12.2 (X = Cl); C 35.7, H 4.5, N 0, S 12.5 (X = Br); C 36.7, H 4.7, N 0, S 12.5 (X = I).

Size exclusion chromatography (SEC)

The molecular weights (M_n) and polydispersity of polymer samples were measured on an Agilent-LC 1200 chromatograph equipped with a PL-aquagel-OH mixed C column and a refractive index detector. 0.7% solution of NaN_3 in deionized water was used as eluent at a flow rate of 1 mL min^{-1}. Calibration was performed using PEO standards (Agilent). Samples of polymer materials were dissolved in deionised water (0.3 mg in 1 mL) and kept for 24 hours prior to analysis to ensure complete dissolution.

Viscometry

The values of relative viscosity (or viscosity ratio) η_r were determined by using an Ubbelohde viscometer at a concentration of 0.05 g dL^{-1} in distilled water at 25 °C. $\eta_r = t/t_o$, where η_r – viscosity ratio, t – average efflux time of solution, and t_o – average efflux time of pure solvent.

Luminescence properties

For emission measurements, the powdered samples were placed between two non-fluorescent glass plates. The absorbance of aqueous solutions of $\{Mo_6X_8\}^{100}$@PSS were set <0.1 at 355 nm. Each solution was poured into two quartz cuvettes and one of them was deaerated by purging with an Ar-gas stream for 30 min and then the cuvette was sealed. The measurements were carried out at 298 K. The samples were excited by 355 nm laser pulses (6 ns duration, LOTIS TII, LS-2137/3). Corrected emission spectra were recorded on a red-light-sensitive multichannel photodetector (Hamamatsu Photonics, PMA-12). For emission decay measurements, the emission was analysed by a streakscope system (Hamamatsu Photonics, C4334 and C5094). The emission quantum yields were determined by using an absolute photoluminescence quantum yield measurement system (Hamamatsu Photonics, C9920-03), which comprises an excitation xenon light source (the excitation wavelength was set at 380 nm), an integrating sphere, and a red-sensitive multichannel photodetector (Hamamatsu Photonics, PMA-12).

Cell culture

All studies were performed in Hep-2 (human epidermoid larynx carcinoma) and HeLa (human uterine cervix carcinoma) cell cultures purchased from the State Research Center of Virology and Biotechnology VECTOR. The cells were cultured in Eagle's Minimum Essential Medium (EMEM, pH = 7.4) supplemented with a 10% fetal bovine serum, 200 mM L-glutamine and 40 μg mL^{-1} gentamicin under a humidified atmosphere (5% CO_2 and 95% air) at 37 °C. A 1 : 2 mixture of 0.25% trypsin solution and 0.02% EDTA solution was used as the medium for cell re-cultivating.

MTT-assay

HeLa or Hep-2 cells were seeded into 96-well plates at a concentration of 5–7 × 10^3 cells per well and then incubated for 24 h under a 5% CO_2 atmosphere at 37 °C. The cells were treated with the solutions of neat PSS and $\{Mo_6X_8\}^{100}$@PSS in

 This journal is © The Royal Society of Chemistry and the Centre National de la Recherche Scientifique 2017

Open Access Article. Published on 05 January 2017. Downloaded on 8/1/2025 11:28:32 AM.
This article is licensed under a Creative Commons Attribution-NonCommercial 3.0 Unported Licence.

the concentration range of 3.2–3300 μg mL^{-1} and incubated for 48 h more under the same conditions. 3-(4,5-Dimethylthiazol-2-yl)-2,5-diphenyltetrazolium bromide (MTT) was then added to each well to a final concentration of 250 μg mL^{-1}, and the plates were incubated for 4 h. The formazan formed was then dissolved in DMSO (100 μL). The optical density was measured using a plate reader Multiskan FC (Thermo scientific, USA) at a wavelength of 620 nm. The experiment was repeated three times on separate days.

Confocal fluorescence imaging

The cells were seeded on microscope slides at a concentration of 1×10^5 cells per slide and incubated at 37 °C under a 5% CO_2 atmosphere for 24 h. The culture medium was then replaced by the culture medium containing 100 μg mL^{-1} PSS or $\{Mo_6X_8\}^{100}$@ PSS (X = Cl, Br or I) and the cells were incubated for 24 h more. The cells were then washed with PBS and fixed in 4% paraformaldehyde. The cells were visualized using a Zeiss LSM 510 confocal microscope (Carl Zeiss Inc., Jena, Germany) equipped with a laser diode (405 nm) for fluorescence and with a 100× oil immersion objective.

Flow cytometry

The cells were incubated with 100 μg mL^{-1} of PSS or $\{Mo_6X_8\}^{100}$@ PSS (X = Cl, Br, I) at 37 °C under a 5% CO_2 atmosphere for 24 h. The cells were then washed with PBS and studied using a FACS Canto II (Becton Dickinson) flow cytometer. A 488 nm excitation source was used with a 695 nm emission filter. All of the data were the mean fluorescence obtained from a population of 10 000 cells. The data were analysed by FlowJo Software.

Evaluation of the photoinduced cytotoxicity

Hep-2 and HeLa cells were seeded in 96-well plates at a density of $5–7 \times 10^3$ cells per well and cultured for 24 h. The cells were then treated with $\{Mo_6X_8\}^{100}$@PSS (X = Cl, Br, I) at concentrations below the dark toxicity (3.2–51.6 μg mL^{-1}) and incubated for 24 h more. After that, the cells were irradiated with a 500 W halogen lamp ($\lambda \geq 400$ nm) for 30 min to apply a total light dose 20 J cm^{-2}. Cells cultured in the medium without $\{Mo_6X_8\}^{100}$@PSS served as the negative control. Cell viability, apoptosis and proliferation were detected by Hoechst 33342/PI staining as previously described by Lee *et al.*[29] In particular, the treated cells and control cells were stained with Hoechst 33342 (Sigma-Aldrich) for 30 min at 37 °C and PI (Sigma-Aldrich) for 10 min at 37 °C. An IN Cell Analyzer 2200 (GE Healthcare, UK) was used to perform automatic imaging of six fields per well under 200× magnification, in brightfield and fluorescence channels. The images produced were used to analyse live, apoptotic and dead cells among the whole population using the IN Cell Investigator software (GE Healthcare, UK).

Statistical analyses

Statistical analyses were performed using the Mann–Whitney U test for unpaired data and P values of less than 0.01 were considered as significant. The data are presented as mean ± SEM (standard error of the mean).

Conclusions

In this work, we have synthesised water-soluble materials $\{Mo_6X_8\}^{100}$@PSS based on a highly ionic polymer, sodium polystyrene sulfonate (PSS) doped by octahedral molybdenum cluster complexes with $\{Mo_6X_8\}^{4+}$ (X = Cl, Br, I) cluster cores and investigated their photoluminescence and biological properties. The materials were obtained by straightforward impregnation of the polymer with the solution of $(Bu_4N)_2[\{Mo_6X_8\}(NO_3)_6]$, complexes with highly labile NO_3^- ligands. The study of photoluminescence showed that the materials based on the $\{Mo_6I_8\}^{4+}$ cluster core showed the highest values of photoluminescence quantum yield and lifetime, and therefore are the most attractive for biological applications.

The study of the biological properties of the materials in Hep-2 and HeLa cells showed that their dark cytotoxicity is noticeably higher than that of PSS, especially in the case of HeLa cells. FACS provided evidence that the treatment of the cells with $\{Mo_6X_8\}^{100}$@PSS led to some uptake of the cluster – at least in the case of the "heavier" (*i.e.* the more emissive) ones – as assessed by the increase of the overall luminescence intensity of the cells. Moreover, materials $\{Mo_6Br_8\}^{100}$@PSS and $\{Mo_6I_8\}^{100}$@PSS also demonstrated some photoinduced cytotoxicity towards HeLa cells. Finally, the overall resistivity of Hep-2 cells towards $\{Mo_6X_8\}^{100}$@PSS was higher than that of HeLa cells.

Acknowledgements

This work was supported by the Russian Science Foundation [grant number 15-15-10006]. O. A. Efremova is grateful to the University of Hull for the academic starting grant. Also, K. A. Brylev thanks the Japan Society for the Promotion of Science for a Post-Doctoral Fellowship for Foreign Researchers.

References

1 M. A. Mikhailov, K. A. Brylev, P. A. Abramov, E. Sakuda, S. Akagi, A. Ito, N. Kitamura and M. N. Sokolov, *Inorg. Chem.*, 2016, **55**, 8437–8445.
2 O. A. Efremova, Y. A. Vorotnikov, K. A. Brylev, N. A. Vorotnikova, I. N. Novozhilov, N. V. Kuratieva, M. V. Edeleva, D. M. Benoit, N. Kitamura, Y. V. Mironov, M. A. Shestopalov and A. J. Sutherland, *Dalton Trans.*, 2016, **45**, 15427–15435.
3 O. A. Efremova, K. A. Brylev, Y. A. Vorotnikov, L. Vejsadova, M. A. Shestopalov, G. F. Chimonides, P. Mikes, P. D. Topham, S. J. Kim, N. Kitamura and A. J. Sutherland, *J. Mater. Chem. C*, 2016, **4**, 497–503.
4 M. N. Sokolov, M. A. Mihailov, E. V. Peresypkina, K. A. Brylev, N. Kitamura and V. P. Fedin, *Dalton Trans.*, 2011, **40**, 6375–6377.
5 K. Kirakci, P. Kubat, M. Kucerakova, V. Sicha, H. Gbelcova, P. Lovecka, P. Grznarova, T. Ruml and K. Lang, *Inorg. Chim. Acta*, 2016, **441**, 42–49.
6 K. Kirakci, P. Kubat, K. Fejfarova, J. Martincik, M. Nikl and K. Lang, *Inorg. Chem.*, 2016, **55**, 803–809.

Open Access Article. Published on 05 January 2017. Downloaded on 8/1/2025 11:28:32 AM.
This article is licensed under a Creative Commons Attribution-NonCommercial 3.0 Unported Licence.

7 K. Kirakci, V. Šícha, J. Holub, P. Kubát and K. Lang, *Inorg. Chem.*, 2014, **53**, 13012–13018.
8 K. Kirakci, P. Kubát, M. Dusek, K. Fejfarová, V. Sícha, J. Mosinger and K. Lang, *Eur. J. Inorg. Chem.*, 2012, 3107–3111.
9 A. M. Cheplakova, A. O. Solovieva, T. N. Pozmogova, Y. A. Vorotnikov, K. A. Brylev, N. A. Vorotnikova, E. V. Vorontsova, Y. V. Mironov, A. F. Poveshchenko, K. A. Kovalenko and M. A. Shestopalov, *J. Inorg. Biochem.*, 2017, **166**, 100–107.
10 Y. A. Vorotnikov, O. A. Efremova, I. N. Novozhilov, V. V. Yanshole, N. V. Kuratieva, K. A. Brylev, N. Kitamura, Y. V. Mironov and M. A. Shestopalov, *J. Mol. Struct.*, 2017, **1134**, 237–243.
11 Y. A. Vorotnikov, O. A. Efremova, N. A. Vorotnikova, K. A. Brylev, M. V. Edeleva, A. R. Tsygankova, A. I. Smolentsev, N. Kitamura, Y. V. Mironov and M. A. Shestopalov, *RSC Adv.*, 2016, **6**, 43367–43375.
12 A. O. Solovieva, Y. A. Vorotnikov, K. E. Trifonova, O. A. Efremova, A. A. Krasilnikova, K. A. Brylev, E. V. Vorontsova, P. A. Avrorov, L. V. Shestopalova, A. F. Poveshchenko, Y. V. Mironov and M. A. Shestopalov, *J. Mater. Chem. B*, 2016, **4**, 4839–4846.
13 C. Neaime, M. Amela-Cortes, F. Grasset, Y. Molard, S. Cordier, B. Dierre, M. Mortier, T. Takei, K. Takahashi, H. Haneda, M. Verelst and S. Lechevallier, *Phys. Chem. Chem. Phys.*, 2016, **18**, 30166–30173.
14 T. Aubert, F. Cabello-Hurtado, M. A. Esnault, C. Neaime, D. Lebret-Chauvel, S. Jeanne, P. Pellen, C. Roiland, L. Le Polles, N. Saito, K. Kimoto, H. Haneda, N. Ohashi, F. Grasset and S. Cordier, *J. Phys. Chem. C*, 2013, **117**, 20154–20163.
15 N. A. Vorotnikova, O. A. Efremova, A. R. Tsygankova, K. A. Brylev, M. V. Edeleva, O. G. Kurskaya, A. J. Sutherland, A. M. Shestopalov, Y. V. Mironov and M. A. Shestopalov, *Polym. Adv. Technol.*, 2016, **27**, 922–928.
16 A. Beltran, M. Mikhailov, M. N. Sokolov, V. Perez-Laguna, A. Rezusta, M. J. Revillo and F. Galindo, *J. Mater. Chem. B*, 2016, **4**, 5975–5979.
17 O. A. Efremova, M. A. Shestopalov, N. A. Chirtsova, A. I. Smolentsev, Y. V. Mironov, N. Kitamura, K. A. Brylev and A. J. Sutherland, *Dalton Trans.*, 2014, **43**, 6021–6025.
18 K. A. Kovalenko, D. N. Dybtsev, S. F. Lebedkin and V. P. Fedin, *Russ. Chem. Bull.*, 2010, **59**, 741–744.
19 D. Dybtsev, C. Serre, B. Schmitz, B. Panella, M. Hirscher, M. Latroche, P. L. Llewellyn, S. Cordier, Y. Molard, M. Haouas, F. Taulelle and G. Férey, *Langmuir*, 2010, **26**, 11283–11290.
20 A. Jensen, F. Basolo and H. M. Neumann, *J. Am. Chem. Soc.*, 1959, **81**, 509–512.
21 http://www.fda.gov/Safety/MedWatch/SafetyInformation/Safety-RelatedDrugLabelingChanges/ucm155126.htm (accessed November 2016).
22 M. A. Mikhailov, K. A. Brylev, A. V. Virovets, M. R. Gallyamov, I. Novozhilov and M. N. Sokolov, *New J. Chem.*, 2016, **40**, 1162–1168.
23 M. N. Sokolov, M. A. Mikhailov, K. A. Brylev, A. V. Virovets, C. Vicent, N. B. Kompankov, N. Kitamura and V. P. Fedin, *Inorg. Chem.*, 2013, **52**, 12477–12481.
24 M. A. Shestopalov, K. E. Zubareva, O. P. Khripko, Y. I. Khripko, A. O. Solovieva, N. V. Kuratieva, Y. V. Mironov, N. Kitamura, V. E. Fedorov and K. A. Brylev, *Inorg. Chem.*, 2014, **53**, 9006–9013.
25 D. A. Basiji, W. E. Ortyn, L. Liang, V. Venkatachalam and P. Morrissey, *Clin. Lab. Med.*, 2007, **27**, 653–670.
26 P. Braack, M. K. Simsek and W. Preetz, *Z. Anorg. Allg. Chem.*, 1998, **624**, 375–380.
27 B. S. Kim, T. H. Fan, O. V. Lebedeva and O. I. Vinogradova, *Macromolecules*, 2005, **38**, 8066–8070.
28 L. Dahne, S. Leporatti, E. Donath and H. Mohwald, *J. Am. Chem. Soc.*, 2001, **123**, 5431–5436.
29 Y. Lee and E. Shacter, *J. Biol. Chem.*, 1999, **274**, 19792–19798.

 This journal is © The Royal Society of Chemistry and the Centre National de la Recherche Scientifique 2017